Materials Advances

ROYAL SOCIETY OF CHEMISTRY

PAPER

View Article Online
View Journal | View Issue

Cite this: *Mater. Adv.*, 2023, 4, 3787

The effect of the TiO_2 interface layer on the electrochromic properties of WO_3-based devices†

Panshu Gui,‡[a] Ziyi Jin,‡[a] Yufeng Bai,[a] Zhengqiao Lv,[a] Jianwei Mo,[a] Shuai Chang [b] and Di Yang *[a]

Herein, using DC magnetron sputtering technology, smooth and dense WO_3 films and WO_3/TiO_2 composite films were successfully prepared under the optimized preparation conditions. Subsequently, electrochromic devices (EC) and photoelectrochemical devices (PEC) were fabricated with a sputtering deposition time of 30 min for the WO_3 film and different deposition times for the TiO_2 interface layer. The TiO_2 interface layers deposited with a sputtering time of 2–3 min were proven to improve the electrochromic properties of the devices. Specifically, compared with the WO_3-based EC devices, the WO_3/TiO_2-based EC devices exhibited a higher transmittance in the bleached sate and much lower transmittance in the coloured state, resulting in a wider transmission modulation range. For instance, the modulation range of the WO_3/TiO_2-based EC devices reached 73.9% at 600 nm, which is larger than that of the WO_3-based EC devices (62.5%). Optical measurements revealed that the TiO_2 interface layer reduced the amount of undesirable localized states by protecting WO_3, while increasing the amount of Li^+ ions embedded in WO_3 for device colouration. This was further demonstrated by cyclic voltammetry measurements. The optimized TiO_2 interface layer significantly increased the inserted Li^+ ion density and extracted Li^+ ion density. Interestingly, the difference between the inserted and extracted charge density was obviously reduced after the introduction of the TiO_2 interface layer. This indicated that the WO_3/TiO_2-based EC devices possessed good cycling stability, which is due to the fact that the surface of WO_3 was passivated by TiO_2, and thus its surface state was not subject to corrosion by the electrolyte and the formation of irreversible interface states was suppressed. Additionally, PEC devices were successfully fabricated based on WO_3/TiO_2 films to investigate their electrochromic characteristics under a small self-driving power. Consequently, driven by the integrated photovoltaic film, the PEC device exhibited a large transmission modulation in the wavelength range from 500 nm to 1800 nm, and especially in the range from 545 nm to 1077 nm, its transmission modulation range exceeded 80%.

Received 30th May 2023,
Accepted 23rd July 2023

DOI: 10.1039/d3ma00272a

rsc.li/materials-advances

Introduction

Electrochromic (EC) devices and photoelectrochromic (PEC) devices[1–3] have been extensively applied in smart windows, heat insulation layers, automobile rearview mirrors that prevent reflected glare, and many other fields. Especially, considering the negative impact of traditional energy consumption on the environment, the development of smart windows that can save energy by adjusting their light transmittance and thermal radiation has become necessary.

To date, tungsten oxide (WO_3) has been intensively studied due to its superior electrochromic properties such as coloration efficiency, stability, low power consumption, good memory effect, and high contrast.[3–5] In recent years, the in-depth research on the electrochromic properties of WO_3 films has accelerated their commercialization.[6–15] Titanium dioxide (TiO_2) is commonly used to enhance the electrochromic performance of WO_3 and achieve photoelectrochromic properties. Early research mainly focused on TiO_2-doped WO_3 films. It was shown that the reversibility of tungsten oxide can be improved by adding TiO_2 to it and the lifetime of TiO_2-doped WO_3 thin films can be several times longer than that of pure WO_3.[16,17] With the development of nanomaterial preparation technology, a variety of WO_3–TiO_2 composite electrochromic materials has been reported, such as WO_3–TiO_2 nanoparticles, porous TiO_2–WO_3 core–shell nanowires, TiO_2–WO_3 core–shell inverse opal structures, and TiO_2/WO_3 hierarchical thin films.[2,17–20] TiO_2–WO_3 electrochromic materials prepared using various technologies have their own

[a] School of Science, Minzu University of China, Beijing 100081, China. E-mail: diyang@muc.edu.cn
[b] Department of Materials Science, Shenzhen MSU-BIT University, Shenzhen, China. E-mail: schang@smbu.edu.cn

† Electronic supplementary information (ESI) available. See DOI: https://doi.org/10.1039/d3ma00272a

‡ Equal contribution.

merits, and once their properties meet the application requirements in the electrochromic field, preparation technology that can achieve large-scale production is particularly favored.

Among the technologies for the preparation of EC devices, the magnetron sputtering method stands out given that the size and composition ratio of the sputtered films can be precisely controlled, the resulting films have high uniformity and good electrochromic performances, and more importantly, it can achieve large-scale production. Several recent reports in the literature showed the indisputable fact that benefiting from the advantages of magnetron sputtering technology, it is expected that ideal EC devices with excellent electrochromic performances and long service lifespans can be prepared.

However, more meticulous and comprehensive research is required to extend the application scope of WO_3/TiO_2-based EC devices fabricated *via* magnetron sputtering. In addition, to date, there is no consensus explaining the mechanism of improving the electrochromic properties of WO_3/TiO_2 using the TiO_2 material, which still has to be explored in detail.

Herein, we report the fabrication of high-quality EC devices and PEC devices based on WO_3/TiO_2 composite films grown *via* DC magnetron sputtering and investigation of the origin of the improvement in device electrochromic properties using a TiO_2 interface layer. In contrast to the WO_3 film-based EC devices, the WO_3/TiO_2-based EC devices possessed a larger transmission modulation range and good cycling stability. Through the combination of quantitative analysis of the localized energy states and driving charge density, we found that the TiO_2 interface layer prompted a reduction in the amount of undesirable localized states, an increase in driving ion density, and an enlargement in the ion diffusion coefficient. This was closely related to TiO_2 protecting WO_3 from electrolyte corrosion, as well as the synergistic effect of energy levels of WO_3 and TiO_2. The WO_3/TiO_2 film was optimized according to these understandings, and consequently, the as-prepared WO_3/TiO_2 devices exhibited a high coloration efficiency of 69 at 600 nm, large-scale transmission modulation range from 500 nm to 1800 nm, and high cycling stability.

Experimental

Materials

Transparent conducting oxide, *i.e.*, fluorine-doped tin oxide (F: SnO_2) in our case, coated glass (FTO) having a sheet resistance of 14 Ω/□ used as the substrate for all experiments. An electrolyte consisting of 0.5 M LiI, 0.05 M I_2, 0.5 M 4-*tert* butylpyridine, and 0.3 M 1,2-dimethyl-3-propylimidazole iodine was dissolved in 3-methoxypropiononitrile to form an high efficiency electrolyte. TiO_2 paste with particle size of 20 nm and N917 dye (Ru(II)L2(NCS)2:2TBA, where L = 2,20-bipyridyl-4,40-dicarboxylic acid) were used to prepare the photovoltaic films. A low-temperature thermoplastic foil with a thickness of 60 μm was used to seal the devices. The above-mentioned materials were supplied by Wuhan Jingge Solar Energy Technology Co. Ltd. A tungsten target and titanium target (99.99% purity, 60 mm diameter and 2 mm thickness) were purchased from Shenyang Baijujie Scientific Instrument Co. Ltd. Anhydrous chloroplatinic acid was obtained from Sigma Aldrich.

Preparation of electrochromic thin films

FTO glass substrates cut in a size of 2 × 3 cm^2 were ultrasonically cleaned in beakers containing acetone, alcohol and deionized water, respectively, for 15 min, and then dried under a nitrogen atmosphere. WO_3 thin films were deposited on the FTO glass substrates *via* DC magnetron sputtering. The distance between the target and the substrate was adjusted to be 18 cm. The working chamber was evacuated to 9×10^{-4} Pa before the deposition of the films. During the deposition of the films, high-purity argon (Ar, 99.99% purity) was used as the sputtering gas, high-purity oxygen (O_2, 99.99% purity) was used as the reaction gas, and the gas flow rate ratio (O_2/Ar) was 1 : 4 and the deposition pressure was 2.0 Pa. The sputtering power was 100 W. The deposition time was set to 30 min after the optimization experiments. The parameters for the preparation of the TiO_2 film by DC magnetron sputtering were the same as that for the WO_3 film, except that the deposition pressure was changed to 5.0 Pa. The deposition time was 1.0 min, 2.0 min, 3.0 min, 4.0 mins, and 5.0 min, and the corresponding samples were named WO_3/TiO_2_1 min, WO_3/TiO_2_2 min, WO_3/TiO_2_3 min, WO_3/TiO_2_4 min, and WO_3/TiO_2_5 min, respectively.

Preparation of platinum thin films

A platinum (Pt) thin film was used as the counter electrode of the devices, which was prepared *via* the spin-coating method. Firstly, anhydrous chloroplatinic acid (H_2PtCl_6) was added to isopropanol and stirred thoroughly to obtain a light yellow transparent liquid with a concentration of 7 mM. Then, the Pt thin film was deposited on FTO glass by spin-coating. The rotational speed was set to 1000 rpm, and the spin-coating time was maintained for 15 s. The prepared samples were dried in an oven at 60 °C for 10 min. To improve the density of the spin-coated film, a second spin-coating was conducted. The electrodes coated with the Pt thin films were gradually heated under an airflow at 100 °C for 30 min, and then at 380 °C for 30 min.

Electrochromic devices assemblage

An EC thin film electrode and Pt-counter electrode were assembled into a sandwich-type cell (Scheme 1) and sealed with a thermoplastic foil with a thickness of 60 μm. The size of the EC thin film was 2.0 cm^2. The aperture of the thermoplastic foil was larger than that of the electrochromic area and its

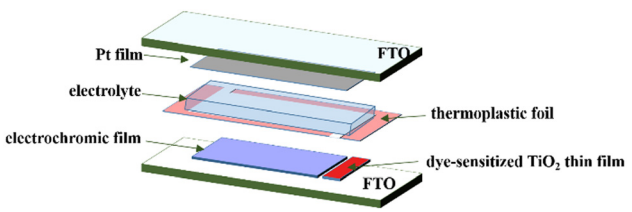

Scheme 1 Configuration of PEC devices.

width was 1 mm. The EC film was fully located in the aperture of the thermoplastic foil. A small hole was reserved at each corner of the thermoplastic foil for injecting the electrolyte. A drop of the electrolyte was put in the hole and it was introduced in the cell *via* vacuum backfilling. The device was placed in a small vacuum chamber to remove the air inside it. Exposing it again to ambient pressure caused the electrolyte to be driven into the device. Finally, the reserved hole was sealed using UV adhesive and the EC device assemblage was completed.

Integration of photovoltaic thin films

A photovoltaic thin film was integrated into the aforementioned EC device to prepare a PEC device that was a self-driving device. The dye-sensitized TiO_2 thin film was used as the photovoltaic film of the PEC device given that its working mode is compatible with that of the EC film. We prepared an EC thin film and the photovoltaic thin film on same electrode of the self-driving device (Scheme 1). Given that high-temperature heat treatment was required for the preparation of the dye-sensitized TiO_2 films, they were prepared before forming the EC films to avoid the influence of heat treatment on the performance of the EC thin films. Moreover, the TiO_2 photovoltaic film covered the smaller area of the electrode. The 20 nm particle-size TiO_2 paste was coated *via* the doctor blade technique and its thickness was controlled using Scotch tape (3 M). The electrode coated with the TiO_2 paste was gradually heated under an airflow at 325 °C for 5 min, 375 °C for 5 min, 450 °C for 15 min, and finally 500 °C for 15 min. Then, the as-prepared TiO_2 films were immersed in a 0.5 mM N-719 dye solution in a mixture of acetonitrile and *tert*butyl alcohol (volume ratio of 1 : 1) and kept at room temperature for 20–24 h to ensure the complete uptake of the sensitizer. After forming the dye-sensitized TiO_2 films, the EC films were prepared through the process described above, and finally the PEC devices were obtained using the same assemblage process as that for the EC device.

Characterization

A field-emission scanning electron microscope (FE-SEM, Hitachi, Ltd, Tokyo, Japan) was used to study the surface morphology of the films. Their optical properties were measured using an ultraviolet-visible-near infrared spectrophotometer (UV-VIS-NIR, Lambda950, Perkin). X-ray diffraction (XRD) measurements were performed on a Bruker/D8 FOCUS X-ray diffractometer (Billerica, MA, USA) with a Cu Kα radiation source (wavelength of 1.5405 Å). Electrochemical performances were tested on an electrochemical workstation (Zahner, Germany). The current density–voltage (J–V) characterizations were carried out on a Keithley 2400 source meter under AM 1.5G simulated sunlight (100 mW cm^{-2}).

Results and discussion

Electrochromic films

The as-prepared WO_3/TiO_2 composite films were smooth and dense, as exhibited by the SEM image (Fig. S1a, ESI†), implying that the TiO_2 thin film was stably and uniformly formed on the surface of the WO_3 film. The XRD pattern of the WO_3/TiO_2 complex film revealed that the as-deposited WO_3 film was amorphous, whereas the TiO_2 film was too thin to display an XRD peak (Fig. S1b, ESI†).

In the case of smart windows, EC films are usually required to be highly transparent in their original state. Thus, we measured the transmission spectra of the individual WO_3 film and WO_3/TiO_2 complex films, as shown in Fig. 1(a). The transmittance of all the samples exceeded 90% for a wavelength greater than 417 nm in the visible light range. Moreover, compared with the WO_3 film, the transmittance of WO_3/TiO_2 complex films showed a slight decrease and significant resonance peaks appeared in the spectrum at a wavelength greater than 600 nm. Our analysis showed that these resonance peaks were the result of the mutual enhancement between the interference of the WO_3 film and that of the TiO_2 film.

To clarify the effect of the TiO_2 layer on the optical property of the EC film, we evaluated the bandgap (E_g) of the individual WO_3 film and WO_3/TiO_2 complex films using Tauc's method, as follows:[21]

$$\alpha(h\nu) = \alpha_0\left[(h\nu - E_g)^n/h\nu\right] \quad (1)$$

$$\alpha(h\nu) = -\frac{1}{d}\ln(T) \quad (2)$$

$$\left[\ln\left(\frac{1}{T}\right)\cdot h\nu\right]^{\frac{1}{2}} = (\alpha_0 d)^{\frac{1}{2}}(h\nu - E_g) \quad (3)$$

where α denotes the absorption coefficient, which is a function of the optical frequency ν, h is Planck's constant, and α_0 is a constant

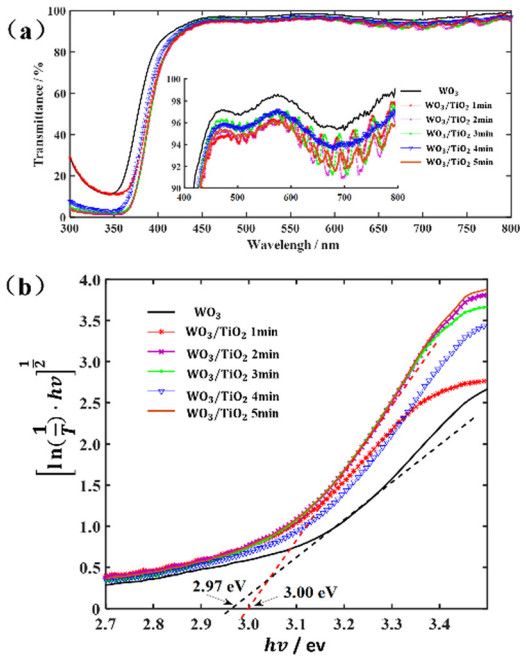

Fig. 1 (a) Transmittance spectra of the individual WO_3 film and WO_3/TiO_2 complex films and (b) curve of $\left[\ln\left(\frac{1}{T}\right)\cdot h\nu\right]^{\frac{1}{2}}$ *versus* $h\nu$.

related to the extent of band tailing. The above-mentioned XRD pattern showed that the prepared WO_3 films were amorphous. Tauc's method is the preferred approach to evaluate the E_g of amorphous (or glassy) materials, in which case n in eqn (1) is taken as 2.[22] α can be conveniently obtained using the transmittance (T) and optical path (d) of the sample (eqn (2)), and therefore eqn (1) can be expressed as eqn (3). According to the curve of $\left[\ln\left(\frac{1}{T}\right)\cdot h\nu\right]^{\frac{1}{2}}$ *versus* $h\nu$, the E_g of the samples was determined by extrapolating the linear least squares fit of $\left[\ln\left(\frac{1}{T}\right)\cdot h\nu\right]^{\frac{1}{2}}$ to zero (Fig. 1b). Obviously, the E_g showed an increasing trend after the introduction of the TiO_2 interface layer. The E_g of the WO_3 film was 2.97 eV, whereas the E_g increased to 3.00 eV for WO_3/TiO_2_5 min.

Electrochromic devices

EC devices were packaged based on the EC films. In the experiment, we found that the a deposition time of more than 3 min for the TiO_2 interface layer led to a decline in the bleaching-colouring performance of the device. Therefore, the samples based on the individual WO_3 film, WO_3/TiO_2_1 min film, WO_3/TiO_2_2 min film, and WO_3/TiO_2_3 min film were mainly explored.

For the proposed ECs, Li_xWO_3 was generated in the WO_3 film, thereby introducing the Li_xWO_3 energy level in the WO_3 energy band, which was reported to be slightly below the conduction band edge (E_C) of WO_3.[23] This means that the localized state just below the E_C of WO_3 is a crucial parameter for exploring the bleaching-colouring performances. Herein, firstly, we investigated the effect of the TiO_2 film on the electrochromic properties through the localized states of the individual WO_3 film and WO_3/TiO_2 composite films.

The localized states below the conduction band (E_C) or above the valence band (E_v) participate in light absorption, which can be represented by Urbach energy (E_U), as shown below:[24,25]

$$\alpha(h\nu) = C\exp\left(\frac{h\nu}{E_U}\right) \qquad ([4])$$

where α, $h\nu$ and C denote the absorption coefficient, photon energy and a constant, respectively. E_U can be obtained from the slope of ln(α) changing linearly with $h\nu$.

The absorption spectra of the WO_3 film and WO_3/TiO_2 composite films in both the bleached and coloured states were measured to explore the changing trend of the localized states (E_U) within their bandgap (Fig. S2a, ESI†). Fig. 2 shows the derived relationship between the function ln(A) and the variable $h\nu$, where A represents the absorbance. Replacing the absorption coefficient with the absorbance did not change the slope of the curve, and therefore it did not change the value of E_U.

For the EC devices based on WO_3, WO_3/TiO_2_1 min, WO_3/TiO_2_2 min, and WO_3/TiO_2_3 min, the values of E_U were 0.298 eV, 0.167 eV, 0.178 eV, and 0.189 eV when the devices were in the bleached state, whereas they increased to 0.384 eV, 0.892 eV, 1.158 eV, and 1.912 eV, respectively, when the devices

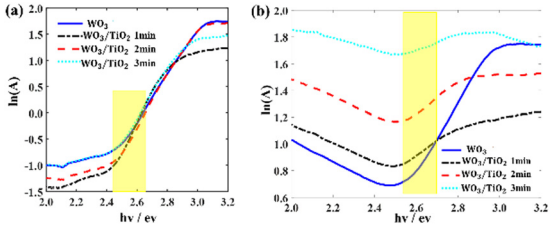

Fig. 2 Relationship between the function ln(A) and variable $h\nu$ from the absorption spectra (a) in the bleached state and (b) in the coloured state. E_U was derived within the yellow range.

were in the colouration state. We considered that the energy level of Li_xWO_3 slightly below the E_C of WO_3[13] was the main contributor to the increase in E_U when the device transitioned from the bleached state to coloured state. Interestingly, under the bleaching condition, the E_U values of all the WO_3/TiO_2 composite films were smaller than that of the individual WO_3 film, whereas under colouration condition, they exhibited a significant increase, even greatly exceeding the E_U value of the coloured WO_3. This indicates that the TiO_2 interface layer reduced the amount of undesirable localized states by protecting WO_3 from electrolyte corrosion and increased the amount of Li^+ ions embedded in WO_3 for device colouration. Undoubtedly, the positive effect of the TiO_2 interface layer enlarged the optical transmission modulation range of the EC devices, which was confirmed by the transmission spectrum and cyclic voltammetry measurements.

The transmission spectra of the EC devices under a driving voltage of +0.6 V and −0.6 V indicated that the TiO_2 surface layer increased the transmittance in the bleached state and reduced the transmittance in the coloured state, thereby increasing the transmission modulation range (Fig. 3a). Taking 600 nm as an example, the modulation range of the WO_3/TiO_2-based EC devices reached 73.9%, which was larger than that of 62.5%

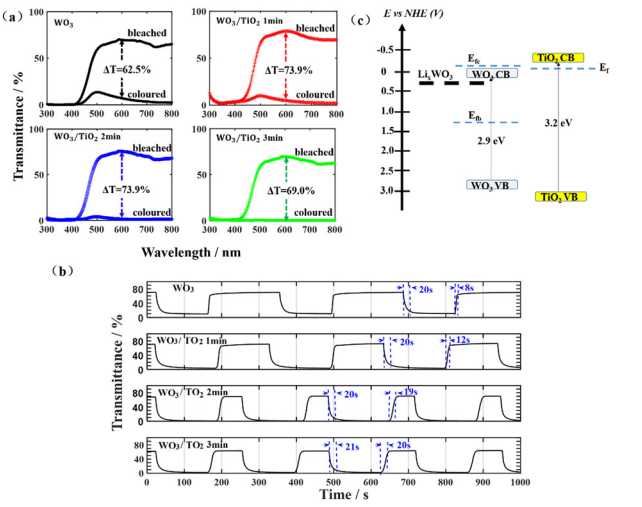

Fig. 3 (a) Transmittance spectra of these EC devices based on the WO_3 film and WO_3/TiO_2 composite films. (b) Bleaching-colouring kinetic measurements at the wavelength of 600 nm under alternating voltaic cycles from −0.6 V to 0.6 V and (c) energy level diagrams for WO_3, TiO_2 and Li_xWO_3.

for the WO_3-based EC devices. The bleaching time and coloration time of these EC devices were revealed by bleaching-colouring kinetic measurements (Fig. 3b). As a reference level to calculate the colouring time or the bleaching time of the device, the highest transmittance in the bleaching state as well as the lowest transmittance in the colouring state of the device were measured. The calculation range of the colouring time is the time it takes to decrease from the highest transmittance to 90% of the lowest transmittance. Similarly, the calculation range of the bleaching time is the time it takes to increase from the lowest transmittance to 90% of the highest transmittance.

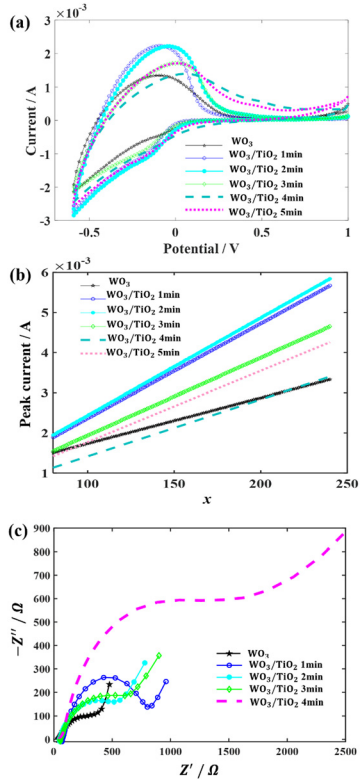

Fig. 4 (a) Cyclic voltammograms between −0.6 V and 1.0 V at a voltaic scan rate of 10 mV s^{-1} for the devices based on the individual WO_3 film and WO_3/TiO_2 composite films. (b) Linear fitting of the peak currents (I_p) and the variables $x = 2.71 \times 10^5 \times S \times n^{3/2} \times D^{1/2} \times C_0 \times v^{1/2}$ at the scan rate (v) of 10 mV s^{-1}, 30 mV s^{-1}, 50 mV s^{-1} and 100 mV s^{-1}. (c) Comparison of the impedance spectra of the devices. The effective area of all the devices was 2.0 cm^2.

Obviously, the TiO_2 interface layer hardly changed the time from bleaching to colouring, which was around 20 s, but it prolonged the time from colouring to bleaching, and the longer the sputtering deposition time of the TiO_2 film, the longer the bleaching time of the device, from 12 s to 20 s. The cause for this phenomenon can be explained by the energy levels, as shown in Fig. 3(c).[26] The Fermi levels of the WO_3 film were represented by two dashed lines to consider the electrochromic state of the film, where E_{fb} and E_{fc} indicate
the Fermi level in the bleached and coloured state, respectively.[27] The relative position of the Fermi level in the coloured WO_3 with respect to the Fermi level of TiO_2 plays a pivotal role in determining the responsivity of the bleaching process.[26] When the E_{fc} of the coloured WO_3 is higher than or close to the E_f of TiO_2, electrons would transfer to the TiO_2 film and be trapped there, resulting in an extension of the bleaching time of the device.

The impact of the TiO_2 interface layer on the electrochromic performance was further explored though cyclic voltammetry (CV) measurements, as shown in Fig. 4(a). By careful observation, it was observed that for the WO_3 film, both the anodic current peak and cathodic current peak were located at −0.097 V. However, upon the introduction of a TiO_2 layer on the WO_3 surface, the anodic peaks shifted towards a positive voltage, while the cathodic peak deviated to a negative voltage. This phenomenon has also been found in a TiO_2 nanotube material decorated with WO_3 particles and WO_3–TiO_2 core–shell nanowires, which was considered to be the synergistic effect of these two materials.[28,29]

The inserted charge density (Q_c) and extracted charge density (Q_b) were recorded by CV measurements, and based on the Q_cs, the coloured efficiencies (CE) of the devices were derived. These physical parameters are summarized in Table 1. Compared with the WO_3-based EC device, the introduction of a TiO_2 interface layer significantly increased the inserted charge density and the extracted charge density. Furthermore, there was a remarkable decrease in the difference between the inserted charge density and the extracted charge density, indicating the improvement effect of the TiO_2 interface layers on the cycle stability of the devices. Combined with the previous analysis of the E_U, we believe that the surface of WO_3 was passivated by TiO_2, and thus its surface state was not subject to electrolyte corrosion, which hindered the generation of irreversible localized states.

In accordance with the optical absorption measurements and the derived charge density, the coloured efficiencies of the

Table 1 The electrochromic properties of the devices based on the individual WO_3 film and WO_3/TiO_2 composite films

Sample name	[a] Q_c/Q_b (C)	Q_b/Q_c (%)	[b] CE at wavelength of 600 nm (cm^2 C^{-1})	D (cm^2 s^{-1})
WO_3	0.0739/0.0669	90.5	31	2.1668×10^{-10}
WO_3/TO_2 1 min	0.1000/0.0977	97.9	28	5.5790×10^{-10}
WO_3/TO_2 2 min	0.1113/0.1066	95.8	35	5.9195×10^{-10}
WO_3/TO_2 3 min	0.0860/0.0816	94.9	69	3.7520×10^{-10}
WO_3/TO_2 4 min	0.1041/0.0889	85.4	—	2.0079×10^{-10}
WO_3/TO_2 5 min	0.1062/0.0981	92.3	—	3.1471×10^{-10}

[a] Q_c or Q_b was obtained in accordance with the CV measurements by the formula $Q = \int_{U_1}^{U_2} I \frac{1}{v} dU$, where v represents the potential scan rate. [b] CE was obtained from the formula $CE = {}^{\Delta a}/_{Q}$, where Δa stands for the optical absorption difference between the coloration state and bleached state.

devices were calculated, as listed in Table 1. There are many physical variables that affect the colouring efficiency, including film thickness, material properties, and driving charge density, and thus it is a multivariable function. In our experiments, the devices based on the WO_3/TiO_2_3 min film had a high coloration efficiency (CE) of about 69 $cm^2\ C^{-1}$.

In addition, based on the CV curves, the diffusion coefficient, D ($cm^2\ s^{-1}$), of Li^+ was calculated using the peak current, I_P, during the anode scans at different scanning rates, as follows:[20]

$$I_P = 2.71 \times 10^5 \times S \times n^{3/2} \times D^{1/2} \times C_0 \times v^{1/2} \qquad (5)$$

where S represents the area of the working electrode material inserted into the electrolyte, C_0 represents the concentration of Li^+ in the electrolyte, $C_0 = 5 \times 10^4$ mol cm^{-3}, and n represents the amount of electrons transferred in the redox process. According to the reaction $3I^- \rightarrow I_3^- + 2e^-$, n was assumed to be 2, and v represents the potential scan rate (V s^{-1}). D can be derived by linearly fitting the current peaks (I_P) in the CV curves (Fig. S3, ESI†) as a function with the variable $x = 2.71 \times 10^5 \times S \times n^{3/2} \times D^{1/2} \times C_0 \times v^{1/2}$ (Fig. 4b), as listed in Table 1. Obviously, the TiO_2 interface layer with an appropriate thickness increased the ion diffusion coefficient. Based on the previous analysis of the localized states and driving charge densities, we believe that the TiO_2 interface layer increased the distribution gradient of active ions in the devices, resulting in a larger ion diffusion coefficient. To comprehensively investigate the effect of the TiO_2 interface layer on the electrochemical performance of the devices, we also measured their impedance spectra, as shown in Fig. 4(c). The TiO_2 interface layers resulted in an increase in the device impedance. The device with the WO_3/TiO_2_2 min film had a relatively reasonable impedance value.

Subsequently, 1000 repeated CV measurements were conducted on the WO_3 device and the WO_3/TiO_2_2 min device to investigate the effect of the TiO_2 interface layer on the device lifetime. Fig. 5a demonstrates that the closed area of the CV curve of the WO_3/TiO_2_2 min device was remarkably larger than that of the WO_3 device, and furthermore Fig. 5b obviously shows that the difference between the inserted and extracted charge density of the WO_3/TiO_2_2 min device was smaller than that of the WO_3 device. Thus, these results indicate that a TiO_2 interface layer with an appropriate thickness is greatly beneficial for improving the lifespan of EC devices.

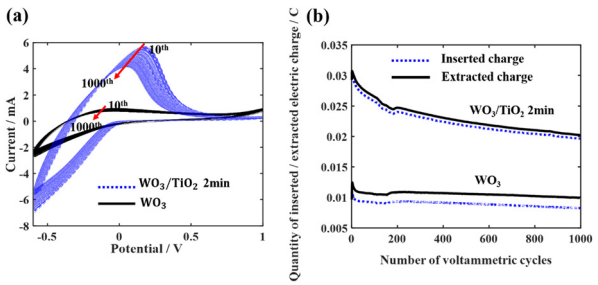

Fig. 5 (a) Cyclic voltammograms for 1000 cycles over the potential range of −0.6 V to 1.0 V at a scan rate of 100 mV s^{-1} for the WO_3/TiO_2_2 min device and WO_3 device. (b) Difference between the inserted and extracted charge density of the WO_3/TiO_2_2 min device and WO_3 device during 1000 CV cycles. The effective area of all the devices was 2.0 cm^2.

Photoelectrochromic devices

We integrated a dye-sensitized TiO_2 thin film into the EC device and constructed a PEC device (Scheme 1). The dye-sensitized TiO_2 thin film, together with the electrolyte and the electrode shared by the EC device formed a photovoltaic cell. Under illumination, the charges generated by the photovoltaic cell directly drove the electrochromic film to change color, and the driving mechanism has been reported in the literature.[30] This driving process avoids energy loss at the joints and in wires when connecting wires externally, and therefore PEC devices can change color sufficiently at a low self-driving energy. To prove this, we investigated the photoelectric conversion efficiency and the electrochromic property of the PEC devices.

The self-driving energy of the PEC device was shown by current density–voltage (J–V) measurements (Fig. 6a). The photoelectric conversion efficiency of the PEC device was very low, *i.e.*, only 1.19%, whereas its fill factor (FF) was high, which indicated that the dye-sensitized TiO_2 thin film possessed a high capacity for doing work.

The variation in the transmittance spectrum of the PEC devices under self-driving energy was investigated in a wide electromagnetic wave range of 400 nm to 2000 nm, as shown in Fig. 6(b). All the tested devices exhibited a high transmission modulation range under very low self-driving energy. In addition, it can be seen that the TiO_2 interface layer increased the transmittance of the PEC devices in the bleached state and enhanced the absorbance of the devices in the coloured state, thereby significantly enlarging the transmission modulation range. Especially for the PEC device based on the WO_3/TiO_2_3 min composite film, the transmission modulation range ΔT exceeded 80% in the wavelength range of 545 nm to 1077 nm. Simultaneously, the coloured PEC device based on the WO_3/TiO_2 film had extremely low transmittance in the near-infrared range, which indicates that this device has promising application prospects in smart windows and heat insulation layers.

Photos of the EC device and PEC device in the initial sate, coloured state and bleached state are shown in Fig. S4 and S5 (ESI†), respectively. To elucidate the advantages of the as-prepared devices, we compared their electrochromic properties

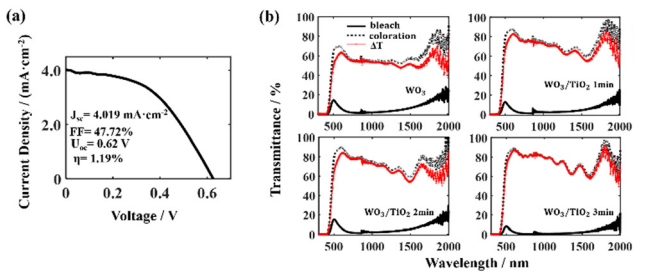

Fig. 6 (a) Current density–voltage (J–V) characterization of the PEC device. (b) Transmittance spectra of these PEC devices based on the WO_3 film and WO_3/TiO_2 composite films, whose transmittance was driven by the dye-sensitized TiO_2 film.

Table 2 The electrochromic properties of various TiO_2/WO_3 composite thin films

	Preparation method	T_b–T_c (%)	Coloration time	CE ($cm^2\ C^{-1}$)	Cycling stability	Production scale	Ref.
WO_3/TiO_2 core/shell nanowires	The method of template and sputtering	41.8/650 nm 72.8/950 nm	30 s	41.6/650 nm 67.4/950 nm	Peak current decreased after 10 cycles	Poor	31
WO_3/TiO_2 Honey-comb films	Anodizing co-sputtered W/Ti films	57.6/550 nm 71.5/633 nm 68.7/800 nm	41 s 550 nm 38 s 633 nm 24 s 800 nm	21.8/550 nm 35.2/633 nm 63.8/800 nm	ΔT did not decrease after 500 cycles	Poor	32
TiO_2/WO_3 core/shell nanoarrays	Hydrothermal method and sol–gel route	16–73	—	—	Peak current decreased after 300 cycles	Poor	33
TiO_2/WO_3 inverse opal structure films	The method of template and dip-coating	65/1033 nm	6 s 1033 nm	111.9/1033 nm	Sustain 90% of the original contrast after 1200 cycles	Poor	19
TiO_2 on WO_3 nanowire arrays	Hydrothermal method and magnetron sputtering	87.0/1500 nm 85.3/633 nm	3 s 633 nm	102.1/633 nm	95.6% after 3000 cycles	Poor	12
WO_3/TiO_2 films	A co-solvent method and spin coating method	62.8/633 nm	3.3 s	57.2/633 nm	The peak current ratio compared with the first cycle are ~80% after CV 1000 cycles	Poor	18
Hierarchical structure WO_3/TiO_2 films	radio frequency magnetron sputtering	80/500–900 nm	30 s	—	Oxidation peak current was no significant change after 1000 cycles	Excellent	20
TiO_2-doped WO_3 films	DC reactive magnetron sputtering	Low	0.55 s	581.39	—	Excellent	34
Devices based on WO_3/TiO_2 films	DC reactive magnetron sputtering	> 80% 545–1077 nm	21 s/600 nm	69/600 nm	Reversibility was no significant change after 1000 cycles	Excellent	This work

with that of various TiO_2/WO_3 composite thin films prepared by representative techniques over the past decade, as listed in Table 2. It is worth noting that due to the lack of research reports on packaged EC or PEC devices based on TiO_2/WO_3 films, the electrochromic properties of the TiO_2/WO_3 films listed in Table 2 were all obtained using electrochemical cells with three electrodes.

Summary

A comprehensive investigation into the electrochromic properties of WO_3/TiO_2-based devices was reported herein. Based on several experiments, the optimal sputtering time range for the TiO_2 interface layer was discovered. The TiO_2 interface layer prepared with a sputtering time of 2–3 min was capable of enhancing the electrochromic properties of the WO_2-based devices significantly. When the TiO_2 sputtering time was less than 2 min, the device performance was not significantly improved, while when the TiO_2 sputtering time was greater than 3 min, the device performance deteriorated, which was manifested as a prolonged response time, and even the inability to change color under a small voltage.

Compared with the WO_3-based EC devices, the EC devices based on the optimized WO_3/TiO_2 film possessed a larger transmission modulation range, higher CE value, superior cyclic stability. Specifically, the WO_3/TiO_2_2 min-based EC device was capable of thoroughly bleaching or colouring driven by a low voltage of 0.6 V, and the bleaching time and the colouring time were 19 s and 20 s, respectively. After 1000 CV measurements, the reversibility of the device had almost no attenuation, as reflected in the extremely small difference between the inserted charge density and the extracted charge density. Driven by the dye-sensitized TiO_2 film, the PEC device based on the optimized WO_3/TiO_2 composite film exhibited a high transmittance in the electromagnetic wavelength range of 500 nm to 1800 nm under the bleaching condition, whereas it had a large absorbance under the colouring condition. Obviously, it possessed a large transmission modulation range, where especially that in the range of 545 nm to 1077 nm exceeded 80%.

Through the quantitative analysis of important physical quantities such as the bandgap (E_g), localized state (E_U), driving charge density, and electrochromic performance, we investigated the mechanism of the TiO_2 interface layer affecting the electrochromic performance of the EC devices. The TiO_2 interface layer significantly reduced irreversible localization states on the WO_3 surface and obviously increased the ion density driving the bleaching-colouring process. These are the main reasons why TiO_2 improved the transmission spectra, transmission modulation range and reversible stability of the EC and PEC devices.

Author contributions

Panshu Gui and Ziyi Jin contributed equally to this work. Panshu Gui fabricated the devices and Ziyi Jin conducted the photoelectrochemical performance measurements. Yufeng Bai, Zhengqiao Lv, and Jianwei Mo measured the electrochromic performance of devices. Di Yang wrote the manuscript. The

authors thank Prof. Shuai Chang from Shenzhen MSU-BIT University for discussion of the device operational mechanism.

Conflicts of interest

The authors declare no competing financial interest.

Acknowledgements

This work was supported by the National Nature Science Foundation of China (22173009, 22211530439).

References

1 C. Bechinger, S. Ferrere, A. Zaban, J. Sprague and B. A. Gregg, Photoelectrochromic windows and displays, *Nature*, 1996, **383**(6601), 608–610.
2 S. Bogati, A. Georg and W. Graf, Photoelectrochromic devices based on sputtered WO_3 and TiO_2 films, *Sol. Energy Mater. Sol. Cells*, 2017, **163**, 170–177.
3 K. Tang, Y. Shi, Y. D. Cui, J. Shu, X. Wang, Y. Qin, Y. Liu, J. Tan, H. HoeWu and Y. Cheng, Fabrication of WO3/TiO2 core-shell nanowire arrays: Structure design and high electrochromic performance, *Electrochim. Acta*, 2020, 330.
4 R.-T. Wen, C. G. Granqvist and G. A. Niklasson, Eliminating degradation and uncovering ion-trapping dynamics in electrochromic WO3 thin films, *Nat. Mater.*, 2015, **14**(10), 996–1001.
5 K.-W. Kim, T. Y. Yun, S.-H. You, X. Tang, J. Lee, Y. Seo, Y.-T. Kim, S. H. Kim, H. C. Moon and J. K. Kim, Extremely fast electrochromic supercapacitors based on mesoporous WO_3 prepared by an evaporation-induced self-assembly, *NPG Asia Mater.*, 2020, **12**(1), 84.
6 P. K. Shen, K. Y. Chen and A. C. C. Tseung, Electrochromism of electrodeposited tungsten trioxide films; 1: Electrochemical characterization, *J. Electrochem. Soc.*, 1994, **141**(7), 1758.
7 K. Tang, Y. Zhang, Y. Shi, J. Cui and Y. Wu, Crystalline WO_3 nanowires array sheathed with sputtered amorphous shells for enhanced electrochromic performance, *Appl. Surf. Sci.*, 2019, **498**, 143796.
8 X. Li, T. YongKim, K.-W. Kim, S. HyunMoon and H. Chul, Voltage-Tunable Dual Image of Electrostatic Force-Assisted Dispensing Printed, Tungsten Trioxide-Based Electrochromic Devices with a Symmetric Configuration, *ACS Appl. Mater. Interfaces*, 2020, **12**(3), 4022–4030.
9 D. Dong, J. Robichaud and Y. Djaoued, Colorimetric Properties and Structural Evolution of Cathodic Electrochromic WO_3 Thin Films, *Can. J. Chem.*, 2021, **99**(6), 549–556.
10 Y. Yao, Q. Zhao, W. Wei, Z. Chen and Y. Gao, WO_3 Quantum-dots Electrochromism, *Nano Energy*, 2019, **68**, 104350.
11 M. A. A, Y. E. F. B, S. R. T. A and A. P. A, Fast electrochromic response and high coloration efficiency of Al-doped WO_3 thin films for smart window applications, *Ceram. Int.*, 2021, **47**(23), 32570–32578.
12 J. Feng, X. Zhao, B. Zhang, Z. Chen, Z. Li and Y. Huang, In situ optical spectroscopic understanding of electrochemical passivation mechanism on sol–gel processed WO3 photoanodes, *J. Energy Chem.*, 2022, **71**, 20–28.
13 M. P. Rodrigues, C. M. Cholant, L. U. Krüger, L. M. Rodrigues and C. O. Avellaneda, A Diffusional Study of Electrochromical Effect and Electrointercalation of Li^+ Ions in WO_3 Thin Films, *J. Electron. Mater.*, 2021, **50**(3), 1207–1220.
14 Y. Cui, Q. Wang, G. Yang and Y. Gao, Electronic properties, optical properties and diffusion behavior of WO_3 with H^+, Li^+ and Na^+ intercalated ions: A first-principles study, *J. Solid State Chem.*, 2021, **297**(S1), 122082.
15 A. Dokouzis, D. Zoi and G. Leftheriotis, Photoelectrochromic Devices with Enhanced Power Conversion Efficiency, *Materials*, 2020, **13**(11), 2565.
16 Z. Wang and X. Hu, Electrochromic properties of TiO2-doped WO3 films spin-coated from Ti-stabilized peroxotungstic acid, *Electrochim. Acta*, 2001, **46**(13–14), 1951–1956.
17 A. Park, Development of WO3 thin films using nanoscale silicon particles, *Jpn. J. Appl. Phys.*, 2000, **39**, 3572–3578.
18 C. Hua, G. Yuan, Z. Cheng, H. Jiang, G. Xu, Y. Liu and G. Han, Building architecture of TiO2 nanocrystals embedded in amorphous WO3 films with improved electrochromic properties, *Electrochim. Acta*, 2019, (309), 354–361.
19 H. Ling, L. P. Yeo, Z. Wang, X. Li, D. Mandler, S. Magdassi and A. I. Y. Tok, TiO2–WO3 core–shell inverse opal structure with enhanced electrochromic performance in NIR region, *J. Mater. Chem. C*, 2018, 6.
20 H. N. Wang, Hierarchical structure WO3/TiO2 complex film with enhanced electrochromic performance, *Solid State Ionics*, 2019, **338**, 168–176.
21 J. Ruska, *Amorphous and Liquid Semiconductors, Proceedings of the Fifth International Conference, Garmisch-Partenkirchen*, Taylor and Francis Ltd, London, 1974, p. 779.
22 A. R. Zanatta, Revisiting the optical bandgap of semiconductors and the proposal of a unified methodology to its determination, *Sci. Rep.*, 2019, 11225.
23 G. Syrrokostas, A. Dokouzis, S. N. Yannopoulos and G. Leftheriotis, Novel photoelectrochromic devices incorporating carbon-based perovskite solar cells, *Nano Energy*, 2020, 105243.
24 F. Urbach, The Long-Wavelength Edge of Photographic Sensitivity and of the Electronic Absorption of Solids, *Phys. Rev.*, 1953, **92**(5), 1324.
25 H. Lee, Y. T. Huang, M. W. Horn and S. P. Feng, Engineered optical and electrical performance of rf–sputtered undoped nickel oxide thin films for inverted perovskite solar cells, *Sci. Rep.*, 2018, **8**(1), 5590.
26 A. Cannavale, M. Manca, F. Malara, L. D. Marco, R. Cingolani and G. Gigli, Highly efficient smart photovoltachromic devices with tailored electrolyte composition, *Energy Environ. Sci.*, 2011, **4**(7), 2567–2574.
27 A. Azens and C. Granqvist, Electrochromic smart windows: energy efficiency and device aspects, *J. Solid State Electrochem.*, 2003, **7**(2), 64–68.
28 N. M. Vuong, D. Kim and H. Kim, Electrochromic properties of porous WO3–TiO2 core–shell nanowires, *J. Mater. Chem. C*, 2013, **1**(21), 3399–3407.

29 Y. Y. Song, Z. D. Cao, J. H. Wang, X. H. Xia and R. Lynch, Multistage Coloring Electrochromic Device Based on TiO2 Nanotube Arrays Modified with WO3 Nanoparticles, *Adv. Funct. Mater.*, 2011, **21**(10), 1941–1946.
30 A. Dokouzis, D. Zoi and G. Leftheriotis, Photoelectrochromic Devices with Enhanced Power Conversion Efficiency, *Materials*, 2020, **13**(11), 2565.
31 N. M. Vuong, D. Kim and H. Kim, Electrochromic properties of porous WO3-TiO2 core-shell nanowires, *J. Mater. Chem. C*, 2013, **1**(21), 3399–3407.
32 Y. Gui and D. J. Blackwood, Honey-Comb Structured WO/TiOThin Films with Improved Electrochromic Properties. 2015.
33 Y. Li, Z. Liu, L. Zhou, T. Cui, B. Wang, K. Guo and J. Han, Titanium dioxide/tungsten trioxide nanoarrays film for high electrochromic performance, *Electrochim. Acta*, 2015, **173**, 117–123.
34 K. Rao, V. C. Babu, V. R. Kumar and N. Veeraiah, Characterization and coloration efficiency studies using cyclic-voltammetry and chronocoulometric methods on TiO2 doped WO3 nanocrystalline thin films, *Optik*, 2022, **249**, 168282.